Performance of Outer-Loop Control for AMC Based on Mutual Information in MIMO-OFDM Downlink

Teppei Ebihara†, Hidekazu Taoka††, Nobuhiko Miki†††, and Mamoru Sawahashi†

†Department of Information Network Engineering, Tokyo City University

††DOCOMO Communications Laboratories Europe GmbH

††† Research Laboratories, NTT DOCOMO, INC.

Abstract

This paper presents the performance of outer-loop control for adaptive modulation and coding (AMC) using mutual information (MI) based mapping between the block error rate (BLER) and received signal-to-interference plus noise power ratio (SINR) in the multiple-input multiple-output (MIMO)-orthogonal frequency division multiplexing (OFDM) downlink employing maximum likelihood detection (MLD). In AMC, we generate a mapping table between the BLER and MI per bit in advance, which is computed from the received SINR, assuming typical channel conditions including the path model and fading maximum Doppler frequency. Then, in the proposed outer-loop control, the measured MI per bit value for selecting the best modulation and coding scheme (MCS) is adjusted so that the measured BLER after turbo decoding satisfies the prescribed target value. Computer simulation results show that the outer-loop control achieves almost the same throughput as that with a mapping table assuming channel conditions identical to those for the actual measurement, while achieving nearly the identical target BLER. Moreover, we show that the best step size, which provides nearly the maximum throughput, differs according to the change in the maximum Doppler frequency in contrast to the relative feedback delay of the AMC loop. Nevertheless, it is insensitive to the target BLER value and frequency-selectivity of a channel model.

I. INTRODUCTION

Commercial service for Long-Term Evolution (LTE) based on Release 8 (hereafter simply Rel. 8 LTE) in the 3rd Generation Partnership Project (3GPP) [1] was launched worldwide with high expectations for real broadband mobile services. In the Rel. 8 LTE downlink, orthogonal frequency division multiple access (OFDMA) was adopted because of its inherent immunity to multipath interference (MPI) due to a low symbol rate, the use of a cyclic prefix (CP), and its affinity to different transmission bandwidth arrangements [2]. In addition, key techniques including scheduling, adaptive modulation and coding (AMC), and hybrid automatic repeat request (ARQ) with soft-combining are essential to achieve efficient packet radio access.

Multiple-input multiple-output (MIMO) channel transmission effectively improves the peak data rate and the received quality by taking advantage of multiple transmitter and receiver antennas [3]. In particular, MIMO multiplexing, i.e., spatial division multiplexing, effectively works to increase the peak data rate of the data channel through the assistance of its robustness against MPI in OFDM radio access. At the receiver, multiple streams are separated by taking advantage of the difference in the propagation channels between the transmitter and receiver antennas. In MIMO multiplexing, different channel-coded streams are transmitted from N_{Tx} antennas, where N_{Tx} denotes the number of transmitter antennas. Moreover, multi-codeword transmission is generally used in MIMO multiplexing. Let N_{CW} be the number of codewords, and N_{CW} is set equal to or less than N_{Tx} (in Rel. 8 LTE, N_{Tx} is 4 and N_{CW} is 2 at maximum). The data rate of each transmission stream belonging to the same codeword is individually controlled when AMC is applied.

In transmission stream-independent modulation and coding scheme (MCS) selection (simply independent MCS selection hereafter), which is generally employed, an MCS is selected individually based on the computed mutual information (MI) [4]-[7] subject to the received signal-to-noise power ratio (SNR) for each transmission stream. In this case, the best MCS, which maximizes the throughput, is selected among the pre-determined MCS candidates while maintaining the target block error rate (BLER) value.

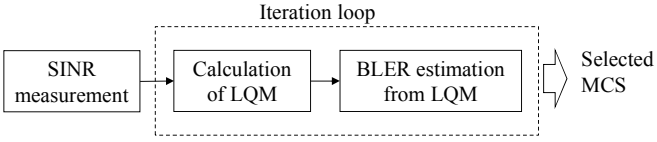

Figure 1. Block diagram of fast AMC.

The AMC operation is performed as shown in Fig. 1. First, the received signal-to-interference plus noise power ratios (SINRs) of the assigned resource blocks (RBs) for all transmission streams are measured using antenna-specific reference signal (RS) symbols. However, in OFDM comprising many subcarriers, the received SINR is different among subcarriers suffering from frequency-selective fading. Signal detection to separate multiple transmission streams depends on the condition-number of the MIMO channel matrix. Hence, a particular pattern of the received SINR over different subcarriers under frequency-selective fading employing specific signal detection affects the achievable BLER. Thus, some link quality metrics (LQMs) were proposed that provide accurate BLER estimations as a function of the received SINR levels including exponential effective SNR mapping (EESM), MI effective SNR mapping, and MI bit mapping [4]-[7]. In a frequency-selected fading channel inducing the received SINR, the mapping function between BLER and the LQM for the *m*-th MCS is approximated as [7]

$$BLER_m(\Gamma) \approx BLER_m^{AWGN}(q(m,\Gamma)) \approx \psi_m(q(m,\Gamma)), \quad (1)$$

where $\psi_m(q(m,\Gamma))$ is the mapping function of the BLER as a function of the LQM and Γ denotes the received SINR. In general, the mapping function, $\psi_m(q(m,\Gamma))$, with the channel coding rate as a parameter is obtained from a Monte Carlo simulation. When ideal channel estimation is assumed, the obtained BLER curve is not subject to a multipath model. However, channel estimation is necessary for coherent detection and SINR measurement. The channel estimation accuracy is subject to a path model including the number of resolved paths. Hence, when the approximation error in (1) is increased, the throughput is degraded and the target BLER is not satisfied. Moreover, since the transmitter is notified of the selected MCS through the control signal in the reverse link, feedback delay is inevitable. Hence, the achievable throughput is degraded and the target BLER is not satisfied due to the feedback delay according to the increase in the maximum Doppler frequency.

This paper presents the performance of outer-loop control for AMC using the MI based mapping between the BLER and received SINR in MIMO-OFDM downlink employing maximum likelihood detection (MLD). In AMC, we generate a mapping table between the BLER and MI per bit in advance, which is computed from the received SINR, assuming typical conditions such as the GSM six-path typical urban (TU) channel model with the fading maximum Doppler

978-1-4673-0990-5/12/$31.00 ©2012 IEEE

frequency of f_D = 5.55 Hz. Then, in the proposed outer-loop control, the measured MI per bit value for selecting the best MCS is adjusted so that the measured BLER after turbo decoding satisfies the target value. The concept of the proposed outer-loop control is identical to that in [8], which assumes the application to High-Speed Downlink Packet Access (HSDPA). The proposed method differs from that in [8] in that the measured MI per bit value for selecting the best MCS in a mapping table between the BLER and MI per bit is adjusted instead of the MCS selection threshold in order to compute an accurate BLER for OFDM under frequency-selective fading conditions. By employing the proposed outer-loop control, almost the identical throughput is achieved to that with the mapping table assuming the same conditions as those in the measurement. The rest of the paper is organized as follows. Section II explains MCS selection with MI based mapping between the BLER and the received SINR applying the proposed outer-loop control. Then, Section III describes the computer simulation configuration. Section IV presents the computer simulation results followed by the concluding remarks in Section V.

II. MCS Selection with MI Based Mapping Using Outer-Loop Control

A. MCS Selection with MI Based Mapping

We assume that the numbers of transmitter and receiver antennas are $N_{Tx} = N_{Rx} = 2$. The number of channel coding blocks, i.e., codewords, is set to $N_{CW} = 2$. In the paper, we use the received SNR over the duration of one subframe as the channel quality indicator (CQI). The received SNR is measured using transmitter antenna-specific orthogonal RS symbols. In the paper, we employ MI based MCS selection [4],[5]. The entire transmission bandwidth is divided into N_{RB} RBs, which is a resource unit to measure the received SNR in the paper. We use RB-common modulation over multiple RBs belonging to the same codeword, which is adopted in the LTE [2]. Here, we assume that all RBs are assigned to the same user. The MCSs of four streams are selected based on the following steps.

1. The received SNR per RB of each transmission stream, $SNR_{m,r}$, is measured as follows (subscripts m and r are the index for the transmission streams, $1 \le m \le N_{CW}$, and the index of RBs, $1 \le r \le N_{RB}$, respectively). The desired signal power of the r-th RB from the m-th transmission stream, $S_{m,r}$, is derived from the channel gain of the respective subcarrier, $\xi_{m,n,s}$, as

$$S_{m,r} = \frac{1}{N_{Sub}} \sum_{s=(r-1)(N_{Sub}/N_{RB})+1}^{r(N_{Sub}/N_{RB})} \sum_{n=1}^{N_{Rx}} \left| \xi_{m,n,s} \right|^2 , \quad (2)$$

where N_{Sub} denotes the number of subcarriers for the entire transmission bandwidth. The noise power is computed from the variance using the channel gains of contiguous subcarriers as

$$N = \frac{1}{N_{Tx} \cdot N_{Rx} \cdot (N_{Sub} - 2)} \sum_{m=1}^{N_{Tx}} \sum_{n=1}^{N_{Rx}} \sum_{s=2}^{N_{Sub}-1} \left| \frac{\xi_{m,n,s-1} + \xi_{m,n,s+1}}{2} - \xi_{m,n,s} \right|^2 \cdot \frac{4}{3} . \quad (3)$$

Then, the received SNR is computed over the duration of one subframe from (2) and (3). Let $\gamma_{m,r} = S_{m,r} / N$ be the instantaneous received SINR of the r-th RB of the m-th transmission stream.

2. Let $I_{k_m}(\gamma_{m,r})$ be the MI value for modulation scheme k_m and $\gamma_{m,r}$ of the m-th transmission stream. The MI value, $I_{k_m}(\gamma_{m,r})$, is computed from the equation given in [4]. Then, the average MI per bit, ρ_{k_m}, is calculated as $\rho_{k_m} = \sum_{r=1}^{N_{RB}} I_{k_m}(\gamma_{m,r}) / N_{RB} B(k_m)$, where $B(k_m)$ is the number of bits per subcarrier of 1 OFDM symbol for the modulation scheme, which is given as k_m = 2, 4, and 6 for QPSK, 16QAM, and 64QAM, respectively.
3. The estimated BLERs for all P MCS candidates are computed from the average MI per bit as $BLER_{h_m} = f_{r_m}(\rho_{k_m})$, where h_m is the MCS index ($1 \le h_m \le P$) and $f_{r_m}(\rho_{k_m})$ denotes the table indicating the BLER performance as a function of the average MI per bit, ρ_{k_m}, with the combination of MCSs comprising modulation scheme k_m and channel coding rate r_m as parameters. In the paper, we derive function table $f_{r_m}(\rho_{k_m})$ by computer simulation for the respective modulation schemes assuming an additive white Gaussian noise (AWGN) channel. The function table, $f_{r_m}(\rho_{k_m})$, is common to all transmission streams and is the same as that for single-antenna transmission.
4. Finally, the most appropriate MCS, MCS_{h_m}, is selected independently based on the computed MI subject to the received SNR for each transmission stream as

$$MCS_{h_m} = \underset{h_m \in B_P}{\operatorname{argmax}} D_{h_m} \{1 - BLER_{h_m}\}, \quad (4)$$

where B_P denotes the MCS set including P MCSs. $D_{h_m} = N_{Sub} r_m B(k_m) / T$ denotes the data rate, which is given as $D_{h_m} = N_{Tx} N_{Sub} r_m B(k_m) / N_{CW} T$, where T is the OFDM symbol duration.

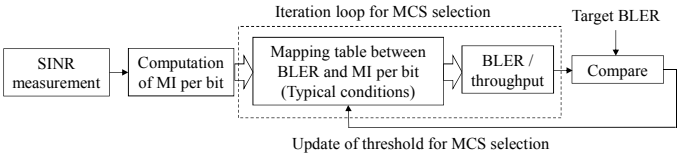

Figure 2. Flow of proposed outer-loop control for AMC in MIMO multiplexing.

B. Outer-Loop Control Scheme

Fig. 2 shows the operational principle of the proposed outer-loop control for the AMC. Figs. 3(a) and 3(b) show examples of function $BLER_{h_m} = f_{r_m}(\rho_{k_m})$, which are used as initial mapping tables for the channel coding rates of R = 1/3 and 3/4, respectively. As aforementioned, the mapping tables are generated in advance assuming typical conditions such as the GSM 6-path TU channel model [9] with the maximum Doppler frequency of f_D = 5.55 Hz, since the radio interface including major radio parameters is optimized at low mobility. As shown in Fig. 3, the achievable BLER is subject to the MCS of other transmission streams as well as that of the stream of interest. Hence, in the outer-loop control we adjust the MCS selection threshold so that the target BLER is achieved. In the proposed outer-loop control, the measured MI per bit value for selecting the best MCS in a mapping table between the BLER and MI per bit is adjusted equivalently to adjust the MCS selection directly to derive the appropriate MCS more simply. Let $\rho_{k_m}(n)$ be the measured average MI per bit at the n-th control interval. Then, the average MI per bit used for selecting the best MCS, $\hat{\rho}_{k_m}(n)$, is updated by the step size Δ_{MI} according to the measured BLER as

$$\begin{aligned} \hat{\rho}_{k_m}(n) &= \rho_{k_m}(n) + \Delta_{MI}, \quad when\ BLER_{measured} \le BLER_{target} \\ \hat{\rho}_{k_m}(n) &= \rho_{k_m}(n) - \Delta_{MI}, \quad otherwise \end{aligned} . \quad (5)$$

In the subsequent evaluations, we employ the common Δ_{MI} value irrespective of the measured $\rho_{k_m}(n)$ value, i.e., modulation scheme and coding rate. Moreover, we measured BLER by moving average with the 100-msec duration in the AMC operation. However, the update for $\hat{\rho}_{k_m}(n)$ based on the measured numbers of ACK/NACK signals instead of the BLER [8] is also applicable.

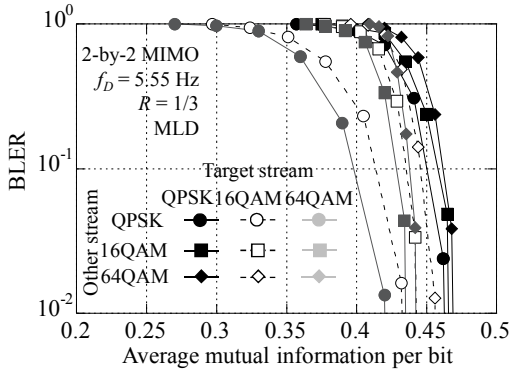

(a) R = 1/3

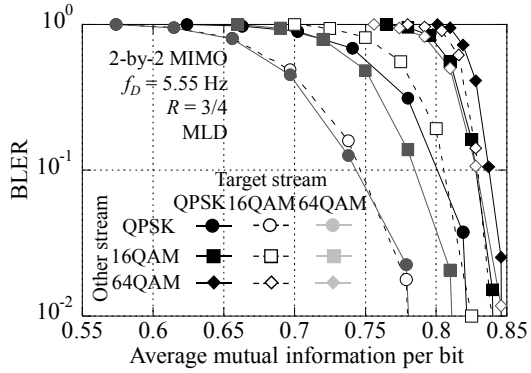

(b) R = 3/4

Figure 3. Example of BLER performance as a function of the average mutual information per bit.

III. COMPUTER SIMULATION CONFIGURATION

Table I gives the major radio parameters used in the simulation. The binary bit sequence is first serial-to-parallel (S/P)-converted into two streams and separately encoded with a turbo code. Variable coding rates in the turbo code are generated by puncturing the mother code with the rate of R = 1/3 and the constraint length of 4 bits. The generator polynomial is set according to that given in [10]. The coded bit sequence is mapped according to the selected modulation scheme. We employ a MCS set that comprises (QPSK, R = 1/3, 2/5, 1/2, 3/5), (16QAM, R = 1/3, 2/5, 1/2, 3/5, 3/4), and (64QAM, R = 3/5, 3/4, 8/9). The feature of the MCS set is that the same modulation schemes are arranged continuously in increasing order of the achievable data rate. In this case, stream-independent MCS selection achieves almost the same throughput as that for joint MCS selection [11]. The symbol sequence is converted into 768-parallel sequences, which corresponds to the number of OFDM subcarriers. Then, the parallel symbol sequences are fed into a 1024-point Inverse Fast Fourier Transform (IFFT) to generate an OFDM signal. The effective OFDM symbol duration is 66.67 μsec and the subcarrier separation is 15 kHz. The resultant entire transmission bandwidth becomes 12.5 MHz. We set 1 subframe to 1 msec, which includes 14 OFDM symbols (FFT blocks). The MCS is updated according to the received SNR at each subframe. Finally, a 4.75-μsec CP is appended to each OFDM symbol to avoid inter-symbol interference.

The received signals are fed to two antennas of a receiver after AWGN is added as receiver noise. Uncorrelated fading variation is assumed between the transmitter/receiver antennas. At the MIMO receiver, ideal FFT timing detection is assumed. Then, after removing the CPs, the received signals are converted into 768 parallel symbol sequences using the FFT. The channel impulse response at each subcarrier position is computed using RS symbols that are multiplexed into the 1st, 5th, 8th, and 12th OFDM symbol positions. In the time domain, we coherently average the channel responses of the two RS symbols within a subframe. Then, the channel response within a subframe is computed every three subcarriers using the RSs. The channel responses between the subcarriers are obtained by coherently interpolating the two channel responses with weighting factors at both ends in the frequency domain. We use MLD signal detection. From the Euclidian distance at the MLD output, *a posteriori* probability (APP) of a symbol including bit "1" or "0" is computed. Finally, the APP is fed into the Max-Log-MAP decoder [12] to recover the transmitted bit sequence through hard-decision for Log-Likelihood Ratio (LLR) at the decoder output.

TABLE I. SIMULATION PARAMETERS

Transmission bandwidth		12.5 MHz
Number of subcarriers		768
Subcarrier spacing		15 kHz
Symbol duration	Effective data	66.67 μsec
	CP	4.75 μsec
Subframe length		1 msec (14 OFDM symbols)
Data modulation		QPSK, 16QAM, 64QAM
Channel coding / Decoding		Turbo coding (R = 1/3-8/9, K = 4) / Max-Log-MAP decoding (8 iterations)
FFT samples		1024
Number of antennas		2-by-2 MIMO
Number of streams		2 streams
Channel model		GSM six-path TU channel model ITU Veh.-A channel model
Symbol timing detection		Ideal
Channel estimation		Interpolation based channel estimation using RS symbols
Signal detection		Full MLD
Feedback delay in AMC		8 msec

IV. COMPUTER SIMULATION RESULTS

We investigate the effect of outer-loop control of the mapping table between the BLER and MI per bit in terms of the throughput and satisfaction of the target BLER using RS channel estimation for various maximum Doppler frequency conditions.

A. Effect of Outer-Loop Control on Feedback Delay

Fig. 4(a) shows the total throughput performance for 2 streams using outer-loop control as a function of the average total received SNR per receiver antenna. The fading maximum Doppler frequency is set to f_D = 55.5 Hz to investigate the effect of outer-loop control on the feedback delay. Fig. 4(b) shows the corresponding average BLER performance assuming the target average BLER of 10^{-2}. In both figures, the performance levels when employing the outer-loop control are plotted as solid lines with the step size as a parameter. The performance levels when using the table assuming the same f_D condition as that in an actual environment, i.e., f_D = 55.5 Hz, are plotted as dotted lines. Hence, the dotted lines represent the influence of the channel estimation error on the table between the BLER and MI per bit when considering the actual Doppler frequency condition. Nevertheless, the influence of the feedback delay for the duration of eight subframes is not considered. Fig. 4(a) shows that the throughput without outer-loop control, i.e., Δ_{MI} = 0, is degraded compared to that assuming the same Doppler frequency condition as in an actual environment. This is due to the RS based channel estimation error and to the feedback delay in the AMC for fast time-varying fading variation. However, by employing the outer-loop control with Δ_{MI} of 0.1, the throughput is significantly improved and almost the identical throughput to that for the actual maximum Doppler frequency condition is achieved. Moreover, from Fig. 4(b), we find that even with the table assuming the same Doppler frequency condition as in the measurement, the average BLER is degraded by approximately one order of magnitude compared to the target value. This is due to

the feedback delay in the AMC loop. The measured BLER without outer-loop control is degraded compared to the target value as well. The outer-loop control with Δ_{MI} of approximately 0.15 achieves almost the same average BLER as the target value. In summary, when the step size of approximately Δ_{MI} = 0.1 – 0.15 is employed in the outer-loop control, the best throughput is achieved while maintaining the target BLER value for f_D = 55. 5 Hz.

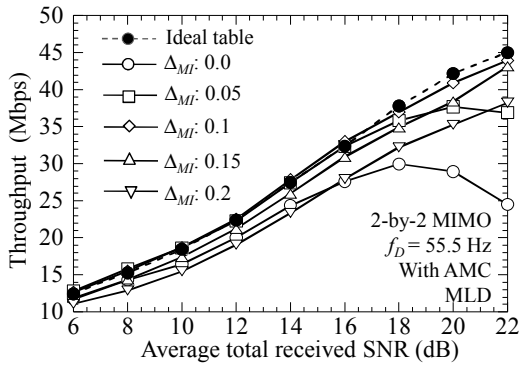

(a) Throughput

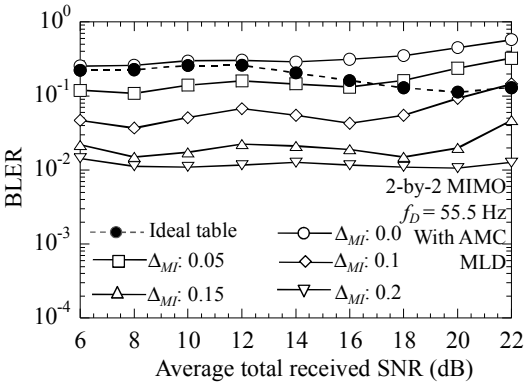

(b) BLER

Figure 4. Performance of outer-loop control for AMC with target BLER of 10^{-2} for f_D = 55.5 Hz and TU channel model.

Next, Figs. 5(a) and 5(b) show the throughput and average BLER performance using outer-loop control in the AMC respectively, as a function of the average total received SNR per receiver antenna for f_D = 222 Hz. Similar to the case in Fig. 4, the dotted line represents the performance based on the table between the BLER and MI per bit assuming f_D = 222 Hz. Clearly, the throughput for f_D = 222 Hz is degraded compared to that for f_D = 55.5 Hz in Fig. 4 due to the increasing relative influence of the feedback delay. In particular, we find that the decoding error in the recovered bits occurs in almost all blocks without outer-loop control when the average received SNR is higher than approximately 14 dB. We see that by using outer-loop control the loss in the throughput is decreased compared to the case employing the mapping table assuming the same maximum Doppler frequency as in the actual condition. The corresponding average BLER approaches the target value. More specifically, almost the best throughput is achieved when the step size in the outer-loop is approximately Δ_{MI} = 0.3 - 0.4, while the measured average BLER approaches the target value. We observe that even applying the outer-loop with the step size of Δ_{MI} = 0.3 - 0.4, the measured BLER is degraded compared to the target value in the high received SNR region. This is because the MCS in which block error does not occur when the instantaneous received signal level drops is selected even after the measured MI value is updated.

From the simulation results, we confirm that the outer-loop control achieves almost the same throughput as that with a mapping table assuming the identical channel conditions to those for the actual measurement, while achieving a nearly identical target BLER. Moreover, the best step size, which provides nearly the maximum throughput, differs according to the maximum Doppler frequency region in contrast to the relative feedback delay in the AMC loop. Hence, the application of different step size values according to the measured $\rho_{k_m}(n)$ value or adaptive step size control according to the rough maximum Doppler frequency region is beneficial to achieving the maximum throughput.

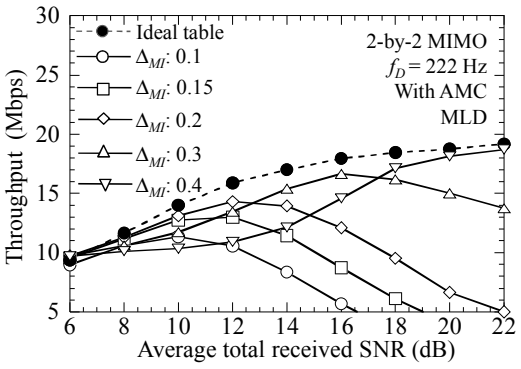

(a) Throughput

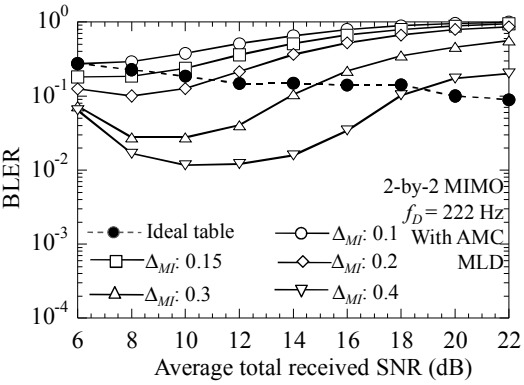

(b) BLER

Figure 5. Performance of outer-loop control for AMC with target BLER of 10^{-2} for f_D = 222 Hz and TU channel model.

B. Influence of Target BLER Values

So far, we have set the target average BLER for outer-loop control to 10^{-2}. Now, we investigate the influence of the target BLER value on the step size in outer-loop control and the resultant throughput. Figs. 6(a) and 6(b) show the throughput performance levels for the target average BLER of 5 x 10^{-2} and 7 x 10^{-2} in the outer-loop control for the AMC, respectively, for f_D = 55.5 Hz. In addition to the throughput with outer-loop control represented as solid lines, the performance using the mapping table assuming f_D = 55.5 Hz is given as a dotted line. We find that for both target average BLERs, the maximum throughput levels are achieved when the step size is approximately Δ_{MI} = 0.1. In this case, almost the same throughput levels are achieved as that for the target average BLER of 10^{-2}. Fig. 7 shows the throughput level for the target average BLER of 5 x 10^{-2} for f_D = 222 Hz. The same tendencies as those in Fig. 6 are observed. Although the overall throughput is degraded according to the increase in the f_D value due to the feedback delay, the best step size, which provides nearly the maximum throughput and simultaneously maintains the target BLER, is almost identical regardless of the target BLER value.

C. *Influence of Propagation Channel Model*

Finally, Fig. 8 investigates the influence of the propagation path model on the target BLER value on the step size in outer-loop control and the resultant throughput. In Fig. 8, we assume the ITU Vehicular-A (Veh.-A) channel model [13], while the mapping tables are generated in advance assuming the GSM 6-path TU channel model. It is assumed that f_D = 5.55 Hz both in the table and the actual measurement. From the figure, even with Δ_{MI} = 0, i.e., without outer-loop control, the measured throughput is almost identical to that for the condition using the mapping tables assuming the Veh.-A channel model. Hence, we see that the influence from the channel model, i.e., channel response in the frequency domain, on the MCS selection is minor when frequency diversity gain is achieved.

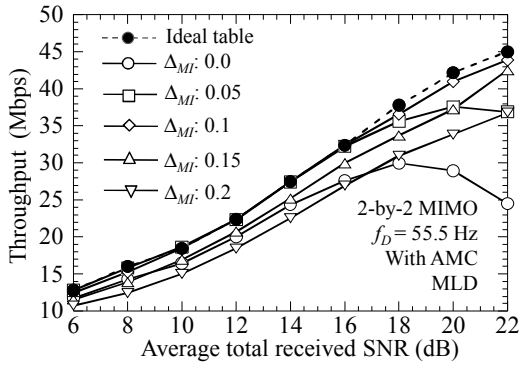

(a) Target BLER of 5 x10^{-2}

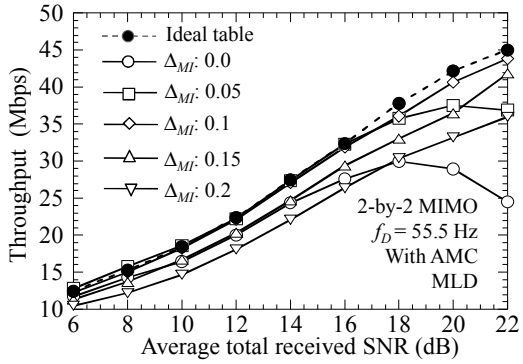

(b) Target BLER of 7 x10^{-2}

Figure 6. Throughput performance of outer-loop control for AMC for f_D = 55.5 Hz and TU channel model.

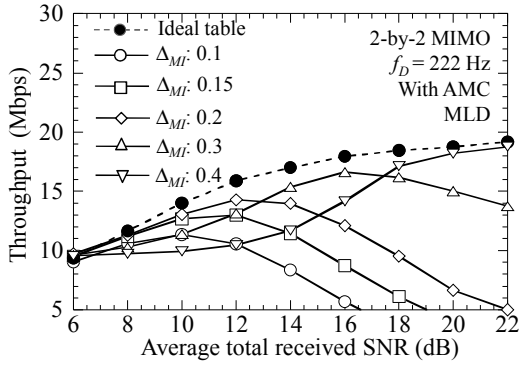

Figure 7. Throughput performance of outer-loop control for AMC with target BLER of 5 x10^{-2} for f_D = 222 Hz and TU channel model.

V. CONCLUSION

This paper presented the performance of outer-loop control for AMC using the MI based mapping between the BLER and the received SINR in MIMO-OFDM multiplexing employing MLD. In AMC, we generate a mapping table between the BLER and MI per bit in advance, which is computed from the received SINR assuming typical channel conditions including the path model and fading maximum Doppler frequency. Then, in the proposed outer-loop control, the measured MI per bit value for selecting the best MCS is adjusted so that the measured BLER after turbo decoding satisfies the target value. Computer simulation results showed that the outer-loop control achieves almost the same throughput as that with a mapping table assuming the channel conditions identical to those for the actual measurement while achieving nearly the identical target BLER. Moreover, the best step size, which provides nearly the maximum throughput, differs according to the maximum Doppler frequency in contrast to the relative feedback delay in the AMC loop. We also showed that although the overall throughput was degraded according to the increase in the f_D value due to the feedback delay, the best step size, which provides nearly the maximum throughput and simultaneously maintains the target BLER, is almost identical regardless of the target BLER value and frequency-selectivity of a channel model.

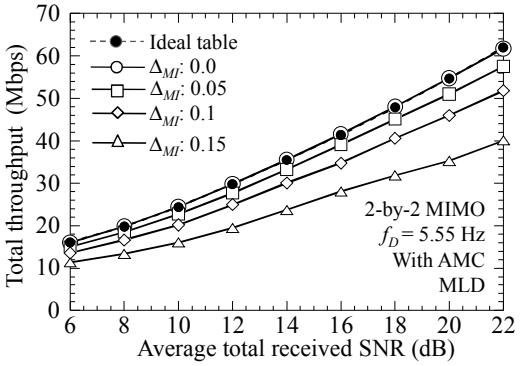

Figure 8. Throughput performance of outer-loop control for AMC with target BLER of 10^{-2} for f_D = 5.55 Hz and Veh.-A channel model.

REFERENCES

[1] 3GPP TS 36.201 (V9.1.0), March 2010.
[2] 3GPP TS 36.211 (V9.2.0), Sept. 2010.
[3] G. J. Foschini, "Layered space-time architecture for wireless communication in a fading environment when using multi-element antennas," Bell Labs. Tech. J., vol. 1, no. 2, pp. 41-59, 1996.
[4] G. Caire, *et al.*, "Capacity of bit-interleaved channels," Electron. Lett., vol. 32, no. 12, pp.1060-1061, June 1996.
[5] N. Miki, *et al.*, "Optimum adaptive modulation and coding scheme for frequency domain channel-dependent scheduling in OFDM based evolved UTRA downlink," IEICE Trans. on Commun., vol. E92-B, no. 5, pp. 1527-1537, May 2009.
[6] T. L. Jensen, *et al.*, "Mutual information metrics for fast link adaptation in IEEE802.11n," Proc. ICC 2008.
[7] T. L. Jensen, *et al.*, "Fast link adaptation for MIMO-OFDM," IEEE Trans. on Veh. Technol., vol. 59, issue 8, pp. 3766 - 3778, Oct. 2010.
[8] J. Lee, *et al.*, "Adaptive modulation switching level control in high speed downlink packet access transmission," 3G Mobile Communication Technologies 2002, pp. 156-159, May 2002.
[9] 3GPP TS 45.005 (V9.4.0), Sept. 2010.
[10] 3GPP TS 36.212 (V8.6.0), March 2009.
[11] T. Ebihara, *et al.*, "Joint MCS selection method for MLD based signal detection in OFDM-MIMO multiplexing with multi-codeword transmission," Proc. WPMC2009, Sept. 2009.
[12] P. Robertson, *et al.*, "A comparison of optimal and sub-optimal MAP decoding algorithms operating in the log domain," Proc. IEEE ICC'95, vol. 2, pp. 1009-1013, June 1995.
[13] "Guidelines for evaluation of radio transmission technologies for IMT-2000," Recommendation ITU-R M.1225, 1997.